Electrical Conductivity of Metal–Polymer Cold Spray Composite Coatings onto Carbon Fiber-Reinforced Polymer

Vincent Bortolussi[1] · Bruno Figliuzzi[2] · François Willot[1,2] · Matthieu Faessel[2] · Michel Jeandin[1]

Abstract Cold spray is a promising process to coat polymers and carbon fiber-reinforced polymer (CFRP). The choice of the metal–polymer couple of materials, however, has a strong influence on coating buildup and properties. In the present work, we show that spraying mixtures of copper and polymer particles lead to composite coating. We observe that the polymer promotes coating buildup onto CFRP to the expense of the electrical conductivity of the coating as a result of its insulating properties. The present work investigates the influence of the coating microstructure on electrical conductivity. Various copper powders, with different morphologies, particle sizes and oxygen contents were mixed with a polyaryl-ether-ether-ketone (PEEK) powder. Cold spray of these powders resulted into composite coatings, and we study the microstructures and electrical properties of such coatings as a function of powder characteristics and spraying parameters. A morphological model of the coating microstructure was developed to reproduce numerically microstructures in 3D. The conductivity of the coatings was measured experimentally for various copper powders. Careful selection of blends of copper and PEEK powders coupled with optimized spraying parameters led to metal–polymer coatings onto CFRP with a fairly high electrical conductivity.

Introduction

The manufacturing of most recent commercial aircrafts involves lighter materials such as carbon fiber-reinforced polymer (CFRP) that replaces aluminum alloys. These materials often combine stacks of carbon fibers embedded in a matrix made of polymer such as epoxy. Unlike aluminum alloys, CFRPs have a high electric resistivity due to the polymer matrix, which prevent current flow to reach the electric discharger. In a lightning impact, such CFRP panels may break and burn, leading to catastrophic failure of the aircraft. To protect them, aircraft manufacturers use lightning screens (metallic meshes) placed on the surface of CFRP panels. Their manufacturing process, however, is complex. To simplify the manufacturing of electrically conductive layer on CFRP, thermal spray processes have been identified as potential solutions. Furthermore, cold spray is, among thermal spray processes, an elegant means for coating CFRP with electrically conductive materials.

Over the past 10 years, a number of studies have been devoted to metallic cold spray coating associated with polymers and composite materials. Several studies are concerned with coating of thermoplastic polymer reinforced with short carbon fibers. In 2006, Sturgeon et al. (Ref 1) achieved dense and adherent cold spray coating of

✉ Vincent Bortolussi
vbortolussi@live.fr

Bruno Figliuzzi
Bruno.figliuzzi@mines-paristech.fr

Michel Jeandin
michel.jeandin@mines-paristech.fr

1   Centre for Materials, Mines ParisTech - PSL Research University, 91003 Evry, France

2   Centre for Mathematical Morphology, Mines ParisTech - PSL Research University, 77300 Fontainebleau, France

aluminum on carbon fiber-reinforced polymer composite materials. In 2011, Zhou et al. (Ref 2) reported difficulties when dealing with cold spray of copper on the same materials. Affi et al. (Ref 3) reported similar difficulties while spraying on carbon fiber-reinforced epoxy.

The CFRP industry uses various types of composites, depending on the material's application and mechanical performance requirements. In particular, the use of short or continuous fibers leads to markedly different microstructures and mechanical properties. Short fibers are dispersed in the matrix, whereas continuous carbon fibers are woven in ply and stacked in the polymer matrix. Moreover, the volume fraction of short fibers in the composite remains low (up to 40%) compared to continuous fibers (up to 70%) (Ref 4). Cold spray of metallic powders on polymers reinforced with short fibers can therefore be assimilated as spraying on polymers: Impacting particles will most often encounter the ductile polymer matrix instead of the short carbon fibers dispersed in it. Upon high-speed impacts of hard metal particles, carbon fibers behave as brittle material and get easily broken. But as the particles mostly encounter ductile polymer, they become embedded in the matrix to form a bond coat, and the coating grows on it. We emphasize that most structural parts of an aircraft body are made with composite materials made of continuous carbon fibers. Accordingly, most metal particles encounter (and break) continuous carbon fibers ply, preventing the bond coat to grow.

A second difference between short and continuous fibers is related to the nature of the polymer matrix. The latter is made of either thermoset polymer, like epoxy, or of thermoplastic polymer, like PEEK. Thermoset polymers exhibit a different behavior upon impact compared to thermoplastic polymers. The first one is not ductile: It breaks upon impact, whereas the second one can absorb various ranges of plastic deformation without failure, depending on its thermo-mechanical properties. Several authors (Ref 5–7) have investigated cold spray materials made from these two types of polymers. Specifically, recent studies focused on metallization of PEEK, because of its applications to many aircraft structures (Ref 8, 9). Malachowska et al. (Ref 10) studied cold spray of metal onto thermoplastic polymer and the electrical behavior of the coatings. They achieved dense and continuous copper coatings on top of PA6 substrates using a tin and alumina interlayers to anchor the copper particles. The resistivity of the coatings reaches 2.6×10^{-7} Ohm m or 3.8×10^{6} S m^{-1}. Also, metallization of carbon fiber-reinforced polymer using cold spray was extensively studied with various methods (Ref 11), but prominently cold spray. Archambault et al. were able to obtain metal coatings using cold spray with a singular but innovative approach in 2016 (Ref 12). They used the mold used to manufacture the composite as a substrate to form a homogeneous although poorly adherent coating which transfers to the composite material during its curing. They obtained dense and adherent copper coatings of various shapes using this method and reported an adhesion of 2.6 MPa and an electrical resistivity of 3.6×10^{-8} Ohm m (or a conductivity of 2.7×10^{7} S m^{-1}). Their solution however circumvents the standing problem of manufacturing cold spray of metal directly onto CFRP. Che et al. (Ref 13) investigated the viability of cold spray of metal particles onto CFRP made with epoxy (thermoset polymer). The authors could not buildup copper or aluminum coatings due to severe substrate erosion; however they found optimized parameters to achieve thick and dense tin coatings on top of the CFRP substrate using a low-pressure cold spray. They presented a buildup mechanism theory, which explains well the differences between cold spray on polymer/composite substrates and on metallic substrates. Using extended investigations, they provided a processing map to achieve tin coatings onto CFRP. These results are highly encouraging and suggest ways of achieving conductive coatings onto CFRP. They however also showed that relatively rigid materials such as aluminum or copper are not suitable as a feedstock. They would erode the substrates without forming any continuous coating, where the softer tin can. These results led the authors to mix tin and zinc, and tin and copper. The tin could deform as it embeds copper, to form a thick and adherent coating (Ref 14).

Experimental results available in these studies could be summarized as follows:

- The mechanical and physical properties of the polymer matrix are very important for manufacturing metallic coatings onto carbon fibers-reinforced polymer using cold spray. Thermoplastic polymer could withstand the impact and deform, whereas thermoset polymers will break. The use of ductile metal may be a viable solution to spray onto reinforced epoxy.

- It is more challenging to obtain thick and adherent coatings onto composite materials with a high-volume fraction of fibers, typically above 50%, than to achieve a coating on materials reinforced with short fibers. Indeed, metal particles cannot deform and anchor to the carbon fibers, and accordingly must encounter polymer for the coating to buildup.

- The deposition window of metal onto polymer is very narrow. Metal particle velocity must be low enough to anchor themselves into the polymer without rebounding, but high enough to allow metal particles to deform upon impact on previously deposited particles. The buildup mechanism is actually a competition between deposition and erosion, as discussed in Che et al (Ref 13).

These observations indicate that thermoplastic polymers could be used as substrates to achieve coatings using highly conductive and rigid powders like copper. Two innovative methods may be used. The first one consists in the deposition of a thin bonding layer made of a thermoplastic polymer onto the CFRP substrate prior to the cold spray of the metallic coating. This layer was however not available for use with cold spray. Instead, the CFRP manufacturer had to add a polymer ply on top of the CFRP panel. In the present work, we focus on a second method: the cold spray of a carefully prepared mixture of polymer and metal powders in order to achieve adherent, conductive and heterogeneous coatings. The metallic part provides the electric properties, whereas the thermoplastic polymer enhances the anchoring of the metal particles and allows the coating to buildup.

The electrical properties of metal–polymer coatings cold-sprayed onto aeronautical grade carbon fiber-reinforced polymers are investigated in the present contribution. Our work focuses on the influence of the heterogeneous microstructure of copper–PEEK coatings on their global (effective) electrical conductivity. The study is divided into three parts:

- First, copper–PEEK powder mix are sprayed at various temperature and pressure to obtain optimal cold spray parameters. Optimal parameters must promote coating buildup as well as conductivity with high copper content.
- Second, the microstructures of the heterogeneous coatings are compared using image analysis in order to improve the understanding of the buildup mechanisms and to determine ways to improve conductivity. We investigate the morphology of the copper phase using image analysis. The modeling and simulation of representative elementary volumes (RVE) of the microstructure are conducted using mathematical morphology theory and numerical tools are presented. Morphological models are useful to determine numerically the physical and mechanical properties of multiphased materials exhibiting periodic or random structures, primarily those of coatings (Refs 15–19).
- Third, the conductivity of the coating is measured. Results are compared to microstructure analysis.

This paper is organized as follows. Details on the materials and processes used are first provided. Results related to cold spray of metal–polymer coatings onto CFRP substrates are then presented, and we study the microstructure of the heterogeneous coatings. We provide then the electrical conductivity measurements and compare them with numerical results. Finally, the results of cold spray parameters optimization, copper microstructure analysis and conductivity measurements are discussed.

Materials

Metal Powders

Three copper powders were sprayed. Their size distribution was measured using a Malvern laser granulometer. The oxide content was measured using Instrumental Gas Analysis by Evans Analytical Group SAS (Tournefeuille, France). These measurements are reported in Table 1, and the loose powders are shown in Fig. 1. The first powder was a high-purity ($\geq$ 99.95 wt.%) spherical copper powder manufactured by TLS Technik GmbH (Bitterfeld, Germany). The second powder was identical to the first powder but with a lower oxide content. It was stored in a sealed container filled with argon. The third powder was made of coarser and irregular particles by POUDMET S.A.S (Bailleval, France). The irregular shape manufacturing process involves oxidation so its oxide content is higher. The three powders are termed, respectively, as oxidized spherical, non-oxidized spherical and irregular.

Polymer Powder

We select PEEK as polymer and mix it with copper. PEEK (polyaryl-ether-ether-ketone) is a semi-crystalline thermoplastic polymer with relatively high temperature properties. It is mainly used in molding applications in the shape of granules. For example, the granules of PEEK 450G from Victrex plc. have a glass transition temperature of 143°C and melt at 343°C. However, as a polymer their mechanical properties decrease quickly as the temperature rises and PEEK then exhibits a high tensile elongation of 45% at 23°C (Ref 20). PEEK is also a dielectric material with a conductivity of 10^{-16} S m^{-1} at 23°C.

Irregular PEEK Vicote 702 powder was obtained from Victrex plc. (United Kingdom). The size of the powder particles ranged from 26.5 μm (d_{10}), to 88.5 μm (d_{90}) with a d_{50} of 52.8 μm. Victrex plc. states that Vicote series powders exhibit the same glass transition and melting temperatures as PEEK 450G.

Copper and PEEK powders were mixed at different volume ratios. The density of copper and PEEK powders were measured using liquid pycnometry to allow precise in-weight mixings.

Substrates

The coatings were sprayed onto carbon fibers-reinforced PEEK of aeronautical grade. Substrate samples of dimension 25 $\times$ 25 $\times$ 2 mm^3 were supplied by Dassault Aviation, Argenteuil (France). The surface of the samples regularly exhibits small bumps made of PEEK matrix on

Table 1 Size distribution of copper powders

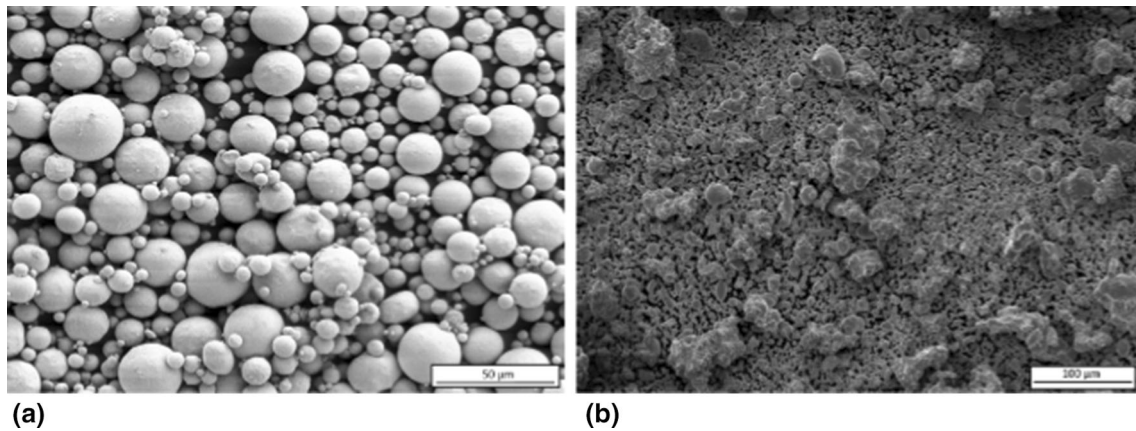| Size Distribution	Oxidized spherical copper	Non-oxidized spherical copper	Irregular copper
D10 (µm)		10.7	11.7
D50 (µm)		19.7	52.8
D90 (µm)		32.8	119.4
Oxide content (ppm)	1100	270	2000

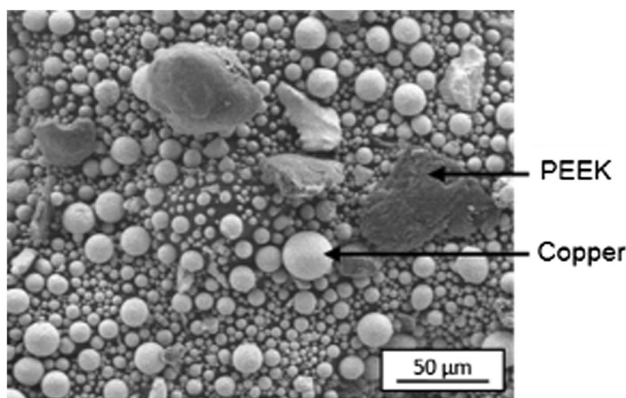**Fig. 1** SEM view of spherical (a) and irregular copper powders (b)

Fig. 2 Optical top view (a), surface profilometry (b) and partial optical cross section (c) of the CFRP substrate

top of the carbon fibers plies and valleys where the fibers would show on the surface, (see Fig. 2).

Samples made of plain Victrex PEEK 450G were also coated. PEEKs in the composite, Victrex 450G and powdered PEEK, were all different. However, a common glass transition of 140°C and a melting temperature of 330°C were considered.

Cold Spray

Spraying experiments were carried out using a KINETICS 3000M cold spray system by CGT-GmbH with a "MOC" nozzle perpendicular to the substrate. The spraying

pressure and temperature ranges available were, respectively, 1–3 MPa and 200–600°C. Standoff distance was kept at 80 mm from the substrate, and all samples were sprayed in one pass only.

Metallographical Observation and Analysis

Coatings were cross-sectioned, polished and metalized using a Cressington sputter coater to be observed with a Leica optical microscope. Metallization greatly enhanced the contrast between the various phases in the microstructure, which improved image analysis. Analyses were performed using ImageJ and the SMIL library (Ref 21), implemented as python scripts. SEM images of the powder were obtained using a ZEISS LEO 1450VP.

Electrical Measurements

The electrical resistance of the coatings was first checked with a mere digital ohmmeter. Then, the electric conductivity of conductive samples was measured using the Van der Pauw method (Ref 22) and a HFS600E-PB4 Linkam four-probe chamber with a Keithley 2450 Sourcemeter. The Van der Pauw method is described in 4.3.

Results

Processing

Cold Spray Parameters Optimization

To increase the electrical conductivity of the coating, we focused on mixtures containing higher volumes of copper, i.e., 80 vol.% and 20 vol.% of PEEK, as shown in Fig. 3. We prepared three mixtures using a tri-dimensional turbulence mixer. The first mixture was made of 80 vol.% of oxidized spherical copper and 20 vol.% of PEEK, the second mixture was made of 80% of spherical non-oxidized copper, and the last one contained 80 vol.% of irregular copper. These mixtures were sprayed onto the CFRP substrates. We investigated the influence of the cold spray parameters, including gas temperature and pressure, for each mixture. The standoff distance, the passing speed and the passing step remained held fixed at the values displayed in Table 2. Coatings were always sprayed in one pass. The optimal parameters were determined by comparing the surface mass of the coating. We estimated the surface mass to be the weight of the coating divided by its surface. The surface of the coating on top of the square

substrate was identified by image analysis techniques. The deposition efficiency could not be calculated due to a lack of precision in the powder flow measurement but can be directly linked to the surface mass of the coatings. The surface mass of the coating was therefore considered to be a simple way to compare the influence of cold spray parameters on the buildup of the coating. Results for the coatings containing spherical, and irregular copper particles are displayed in Figs. 4 and 5, respectively.

The optimal gas temperature and pressure for the mixture containing 80% of spherical oxidized copper are 400°C and 1.5 MPa, as they led to a higher surface mass therefore higher deposition efficiency, as shown in Fig. 4.

Table 2 Cold spray parameters

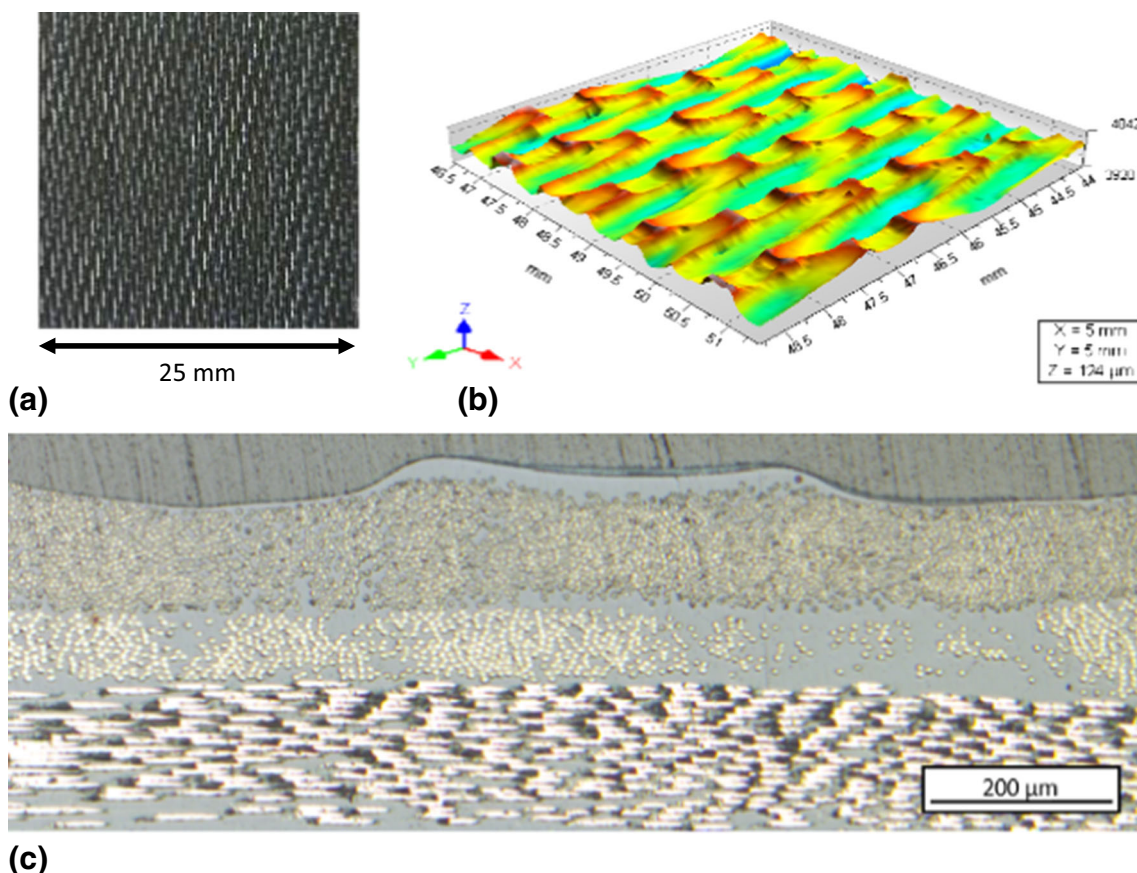| Cold spray parameters	
Gas temperature	300–500°C
Gas pressure	1.0–2.0 MPa
Standoff distance	80 mm
Passing speed	100 mm s^{-1}
Passing step	1 mm

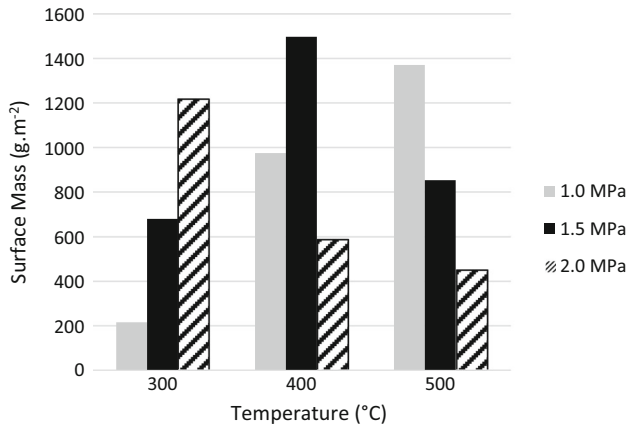Fig. 3 SEM view of a spherical copper–PEEK powder blend

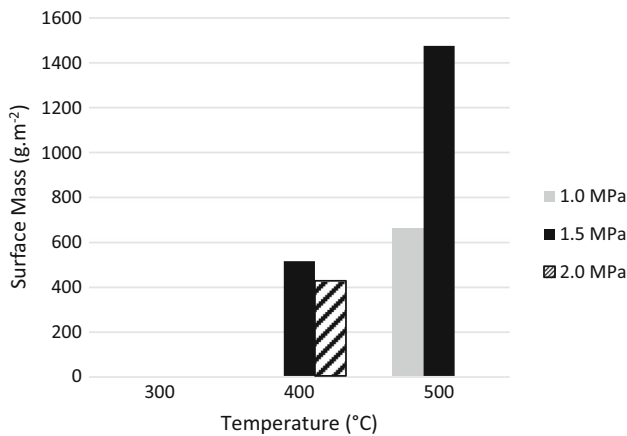**Fig. 4** Surface mass of the coatings containing oxidized spherical copper depending on gas temperature and pressure

Fig. 5 Surface mass of the coatings containing irregular copper depending on gas temperature and pressure

Fig. 6 Influence of cold spray parameters on the surface of coatings with oxidized spherical copper

Fig. 7 Surface mass of coatings with oxidized and non-oxidized copper sprayed at different passing speeds

They were found to be identical for spherical non-oxidized copper. The influence of the parameters on the buildup and surface aspect of these coatings are shown in Fig. 6. Coatings sprayed at 300°C exhibited very poor adhesion, with several uncoated and eroded area (black spots). A pressure of 2 MPa had the same effect, especially at temperatures of 500°C. The best results were obtained at 1–1.5 MPa and 400–500°C, where the coatings appeared homogeneous and thick, demonstrating a good buildup and adhesion of the particles to the CFRP substrate. The semicircular black zones on top of the samples are the marks of the fixation rings that hold the substrates during spraying.

For the highest values of temperature and pressure, the impacting particles mostly broke the carbon fibers and bounced, leaving an eroded substrate with a few coated zones, as shown in Fig. 6. These coated zones correspond to the bumps of PEEK whence the coating could more easily grow. In contrast, this could not occur in the valleys due to the presence of brittle carbon fibers, as shown in Fig. 2(c). The optimal parameters led to a homogeneous
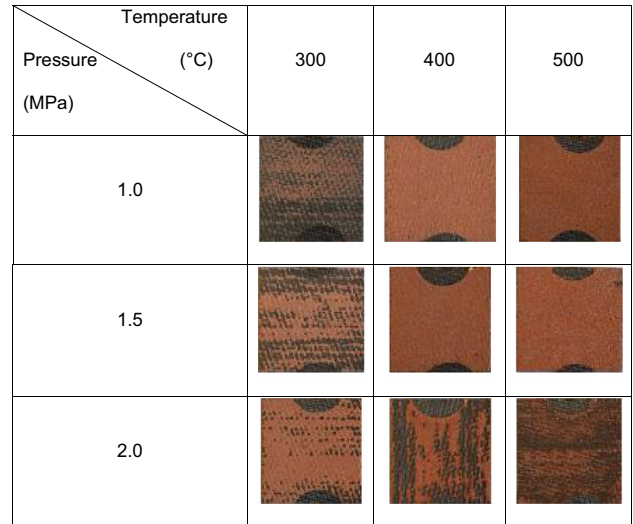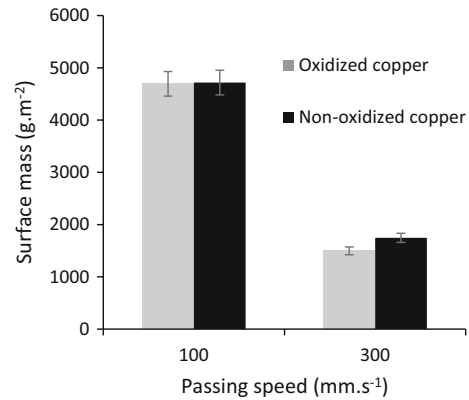
surface where the bumps and valleys of the substrate were reproduced on the coating. Regarding the mixture made from irregular copper powder, as shown in Fig. 5, although the optimal parameters were shown to be 500°C and 1.5 MPa, subsequent coatings were sprayed at 400°C and 1.5 MPa, as the CGT 3000 cold spray could hardly stabilize the gas flow at 500°C and 1.5 MPa. At 300°C or at 500°C and 2.0 MPa, this mixture did not lead to any coating, but to substrate erosion only, as shown in Fig. 5.

Coatings with non-oxidized spherical particles were sprayed with the optimized parameters, namely 400°C and 1.5 MPa for spherical particles, at 100 mm s^{-1} with a passing step of 1 mm. Their surface mass was compared to the same coatings containing oxidized spherical particles, as shown in Fig. 7. They appeared to be almost identical. Similar experiments were carried at 300 mm s^{-1} with a passing step of 1 mm. The surface masses were slightly

different but still close. Consequently, oxidation on the spherical particles has a negligible influence on coating buildup.

Even if the influence of oxidation on the buildup is negligible, one should however notice that it remains very sensitive to the shape of the particles. Using spherical copper particles, a pressure of 1.5 MPa therefore seems to constitute a good compromise. At 1.0 MPa, increasing the temperature leads to higher coating surface mass, but the reverse at 2.0 MPa. It can thus be assumed that temperature and pressure have opposite effects on PEEK and copper, respectively. Therefore, there is a very narrow window for which both lead to higher deposition efficiency. Regarding irregular particles, the results are bolder: It mostly only works at 1.5 MPa and 500°C.

Processing of Samples for Electric Measurements

The coatings used for electrical measurements were all sprayed at 400°C and 1.5MPa, whereas the passing speed and step were only modified to adjust the coating thickness.

Coating samples for electric conductivity measurements were sprayed onto the thinner (< 1 mm) PEEK substrates for investigation into their electrical behavior using the Van der Pauw method. These coatings were sprayed onto a PEEK substrate instead of CFRP to prevent any influence of conductive carbon fibers interference in electrical measurements. Carbon fibers are good electrical conductors actually for a metallic coating onto CFRP, if the coating is in direct contact with carbon fibers the current could partially flow through them thus leading to false measurements.

To ensure that the coatings sprayed onto PEEK were similar to those sprayed onto CFRP, we investigated the influence of the substrate on the coating thickness and copper ratio. Thick samples were sprayed onto PEEK and CFRPs. Thickness and copper ratio were measured using image analysis of cross sections of 5 random images (2560×1920 pixels^2 with one-pixel side being of 0.242 µm). Results are summarized in Table 3. Through these measurements, the coating morphology appears mostly non-dependent of the substrate. Coatings thicknesses are

similar, and copper surface fraction appears slightly higher for the PEEK substrate. It may actually be higher, because the copper particles can easily anchor on plain PEEK, better than on the PEEK matrix of the composite substrates.

Microstructure of the Cu–PEEK Coatings

Microscopic Observation

Thick coatings made of the three mixtures and sprayed with the optimal parameters onto CFRP were cross-sectioned and observed for their microstructure to be analyzed qualitatively and quantitatively.

The coating morphology for oxidized spherical copper, non-oxidized spherical copper and irregular copper is shown in Fig. 8(a), (b) and (c), respectively. The copper particles are bright, whereas the PEEK resulted in a gray matrix. The black holes correspond to debonded particles during preparation of the cross sections. Although the materials are initially the same, the microstructures are actually different, which highlights the effect of oxidation and shape on the deformation of copper. In the microstructure made of oxidized spherical copper, the metal particles can be clearly identified. They globally kept their spherical shape as a consequence of low deformation upon impact. Moreover, most of the particles appear outlined by PEEK. If not, the boundaries between adjacent particles are still visible, unlike what can be seen in conventional cold spray metallic coatings. By contrast, non-oxidized particles are mostly bonded together and some are heavily deformed. For many of them in contacts, the location of their boundaries could not be distinguished, demonstrating a strong bonding. A magnified cross section is shown in Fig. 19. As the spherical particles are the same, except for their surface oxide content, this highlights the oxidation effect on the particle ability to deform and bond. The irregular particles appear to be also quite bonded but still with some PEEK interlayers. Their dendritic shape might locally induce a higher deformation than for spherical copper.

Table 3 Comparison between coatings sprayed on PEEK and CFRP substrates

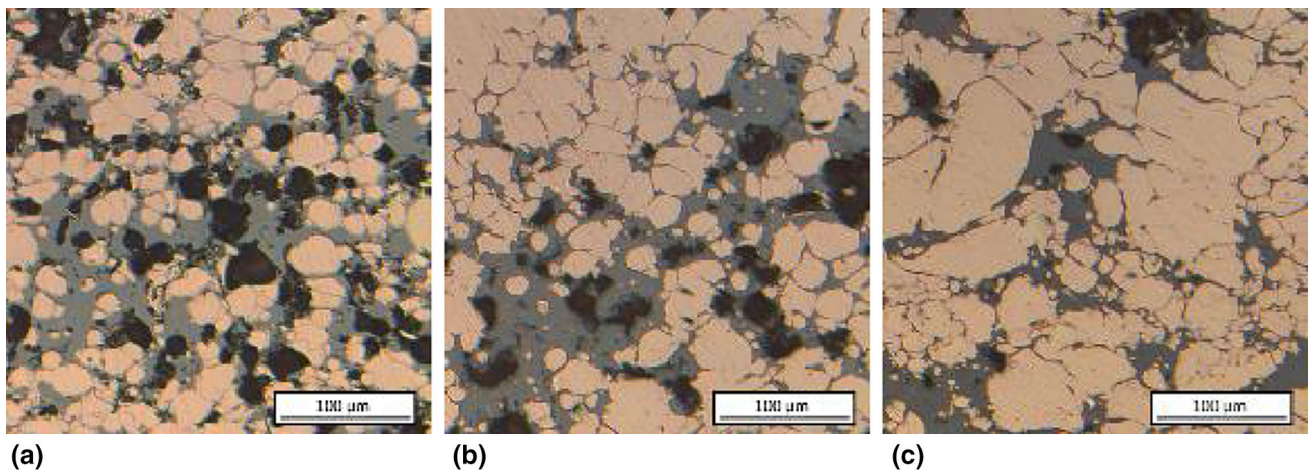| Powder mixture	Substrate	Coating mean thickness (µm)	Copper surface percentage (absolute standard deviation)
80 vol.% non-oxidized spherical copper—20 vol.% PEEK	PEEK	1058 ± 21	73% ± 4%
	CFRP	1037 ± 31	69% ± 4%
80 vol.% irregular copper—20 vol.% PEEK	PEEK	781 ± 23	72% ± 4%
	CFRP	739 ± 29	69% ± 4%

Fig. 8 Optical cross section view of Cu–PEEK composite coatings with (a) spherical oxidized, (b) non-oxidized and (c) irregular copper

Table 4 Morphological characteristics of the microstructures

Copper initial ratio	Copper powder in the mixture	Copper mean surface fraction absolute standard deviation)	Inter-particular contacts ratio (%)
80%	Spherical oxidized	66% $\pm$ 3%	73
	Spherical non-oxidized	69% $\pm$ 5%	70
	Irregular	69% $\pm$ 4%	68

In all three microstructures, PEEK embeds the copper particles. Moreover, the copper surface content is different from the volume content. However, the volume content of copper needs to be as high as possible to achieve a higher conductivity. It is assumed that above a certain "threshold volume," copper could form a network in the coating, which allows the passage of the current. The problem is that PEEK filled the interstices between copper particles. The layers separating the copper therefore lower the conductivity by preventing the current from flowing through a copper network. Hence, the contacts between the particles are a key characteristic of the microstructure morphology. The ratios of particles in contacts as well as the copper volume content are believed to govern the conductivity of the coatings.

With the objective of attaining a higher electrical conductivity, the study focused on the morphology of the copper phase, the copper content and the existence of a path for the current to circulate through the microstructure. The two main morphological characteristics that were extracted from the images were the copper surface fraction (assumed to correspond to the volume ratio due to the shape and the number of particles) and the ratio of contacts between particles. They were extracted from 13 random images (2560×1920 pixels^2 with 1 pixel = 0.242 µm) of each sample through a specifically developed segmentation procedure. The results are summarized in Table 4.

In fact, the image scale was too large for the analyses to be accurate enough, mainly for inter-particular contacts. The boundaries of the particles were not so well defined in the images, which made sometimes the segmentation process not suitable for distinguishing two particles. Despite this drawback, this scale was kept to work on representative samples with a large number of particles. More precise images would require much more memory and a longer segmentation time.

These analyses show that the microstructures containing irregular and non-oxidized particles reach a copper surface fraction of 69%, not far from the 66% for the microstructure made of oxidized particles. Assuming that the images were representative due to the high number of involved particles, the surface fraction was taken equal to the volume fraction. The difference between microstructures was rather slight, but all of them exhibited a copper content below the initial volume content of 80%. The difference is believed to come from particles that rebounded due to their higher velocity or their inability to deform and anchor. Regarding the particles in contact, the segmentation process could only hardly identify most of the irregular or spherical oxidized particles, as shown in Fig. 9. Actually,
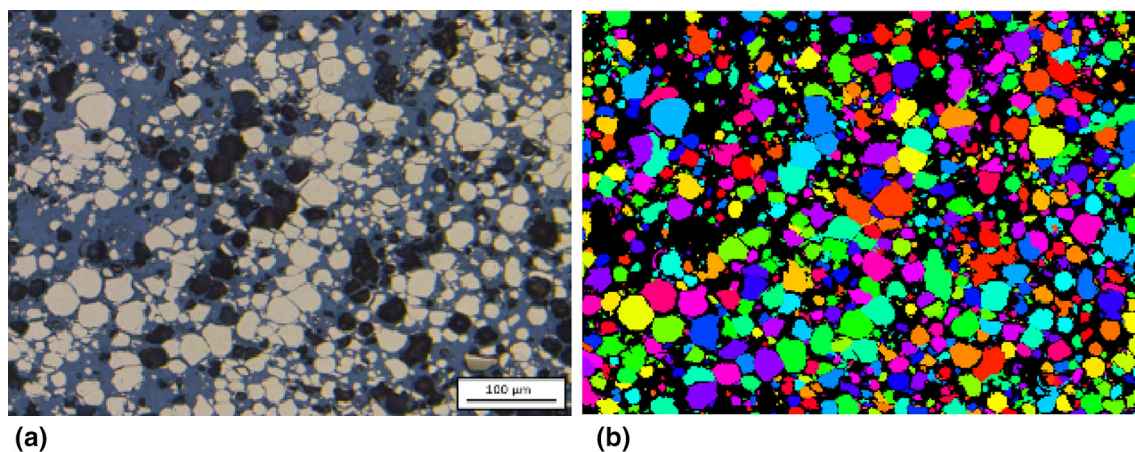
Fig. 9 Original (a) and overspreading segmented images with labeled particles (b)

the limitation of the process was reached when processing irregular particles due to their bigger size and the fact that their boundaries were not outlined enough. The absence or the difficulty to identify the boundaries between non-oxidized particles prevents the process to precisely compute the number of contacts in these microstructures. The interparticular contact ratios for these coatings could therefore be rather incorrect. However, this mere fact also confirmed that the particles were strongly bonded, which promoted the electric conductivity.

3D Numerical Simulation of the Microstructure

Based on microscopic observation, we decided to investigate numerically the influence of the microstructure and its morphological characteristics on conductivity in 3D samples. X-ray microtomography could not result in 3D volumes of the samples due to materials heterogeneity and physical properties. Hence, following a common approach in material engineering (Refs 23, 24), we developed a morphological model of microstructure to simulate 3D microstructures.

The morphological model is a two-scales model, where the first scale is a Boolean model which represents the copper particles as spheres that were randomly generated in a 500 voxels^3 volume through a Poisson point process. Each sphere has a radius randomly sampled through a Gamma law. The spheres can overlap, which leads to randomly generated aggregates.

The second scale of the model corresponds to PEEK interstices between the particles, generated using a modified Johnson–Mehl model. Nuclei are generated in locations corresponding to the barycenters of the aggregates of spheres. For each nucleus, a cell propagates in 3D through the aggregate. The cell growth is simulated using the Eikonal equation (Ref 25). When two cells meet, they stop

growing and their contact surface is transformed into a volume filled with PEEK with a randomly generated thickness sampled from an exponential law. Using various propagation rates tend to create roughly flat separation volumes between particles, as shown in the experimental images, as shown in Fig. 10(a) and (b).

The parameters of the two-scales model were optimized by fitting two morphological characteristics, which were measured in the experimental images and cross sections of the simulated microstructures. These two characteristics are the covariance and the granulometry of the copper phase. The covariance is defined as the probability for a random point in a given aggregate, to remain in the aggregate after a displacement from a vector **r** in a given direction. Increasing the norm ‖**r**‖ of the vector allows to create a chart of the covariance, as shown in Fig. 11(a). It is defined as:

$$C(r) = P\{x \in H, x + r \in H\}, \qquad (Eq\ 1)$$

where H is the union of the copper particles in the coating, x some point in the observation window, and r some vector in R^2. The cumulative granulometry is calculated by eroding the copper phase with a probability:

$$G(s) = \frac{P\{x \in H\} - P\{x \in H(S, s)\}}{P\{x \in H\}}, \qquad (Eq\ 2)$$

where x is a point in the observation window, H is the copper phase and $H(S; s)$ is the morphological erosion of H by a square S of side length s, as shown in Fig. 11(b).

The simulation was also used to simulate microstructure containing non-oxidized copper, leading to similar results, as shown in Figs. 12(a), (b) and 13(a), (b).

This approach allowed to numerically reproduce volumes in the microstructure that are similar to the experimental observations and yield similar covariance and granulometry.
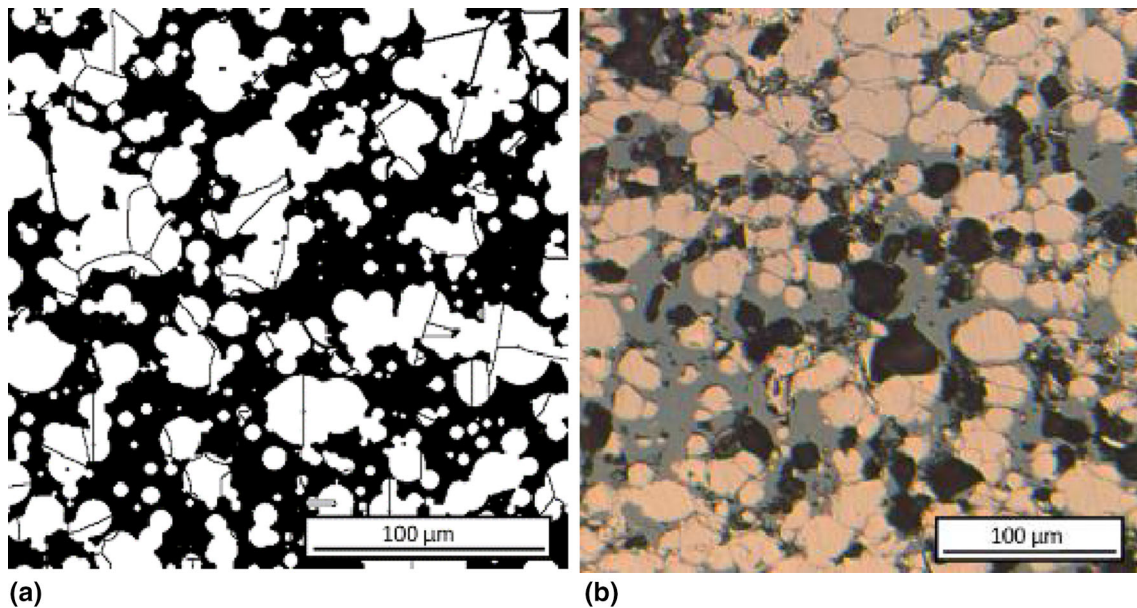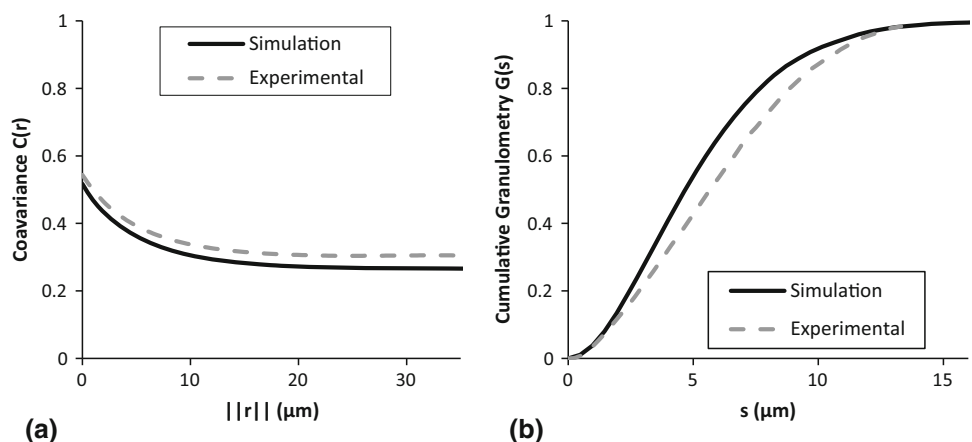
Fig. 10 Simulated (a) and experimental (b) images of a microstructure made of PEEK + oxidized copper

Fig. 11 Mean covariance and granulometry of the experimental and simulated microstructures with oxidized copper

Numerical volumes were simulated for microstructures containing spherical oxidized and non-oxidized copper. The scale of the numerical volumes was enlarged at 1 voxel side = 0.484 μm for reducing the computation time and the volumes to be representative enough. The simulated volumes were $500 \times 500 \times 500$ voxels periodic cubes containing a non-percolating copper phase. For each type of microstructure, 5 volumes were simulated.

Electrical Measurements on Coatings

Samples made of each one of the three mixtures containing 80% (vol.) of copper and 20% (vol.) of PEEK were achieved using optimal cold spray parameters. For each type of mixture, two samples of different thicknesses were sprayed onto PEEK substrates. The conductivity of each sample was first tested with a portable ohmmeter, and it

quickly appeared that the coatings with spherical oxidized copper were fully insulating. Hence, the study focused on coatings with spherical non-oxidized and irregular copper powder. Two methods were identified to measure the conductivity of the coating: the four-probe sensing method and the Van der Pauw method (Ref 22). The four-probe method is the classic approach in which a current is applied along a line of the sample, and the resulting resistance is measured (Ref 26). However, it is mostly suitable for thick and homogeneous samples of well-known size. The Van der Pauw method is also based on resistance measurements but is more suitable for 2D samples, i.e., for samples with a dimension much smaller than the other. Moreover, it gives an average measure of the conductivity where the four-probe sensing method yields the conductivity in one direction. Thus, we opted for the Van der Pauw method, assuming that our coatings met the required criteria. The
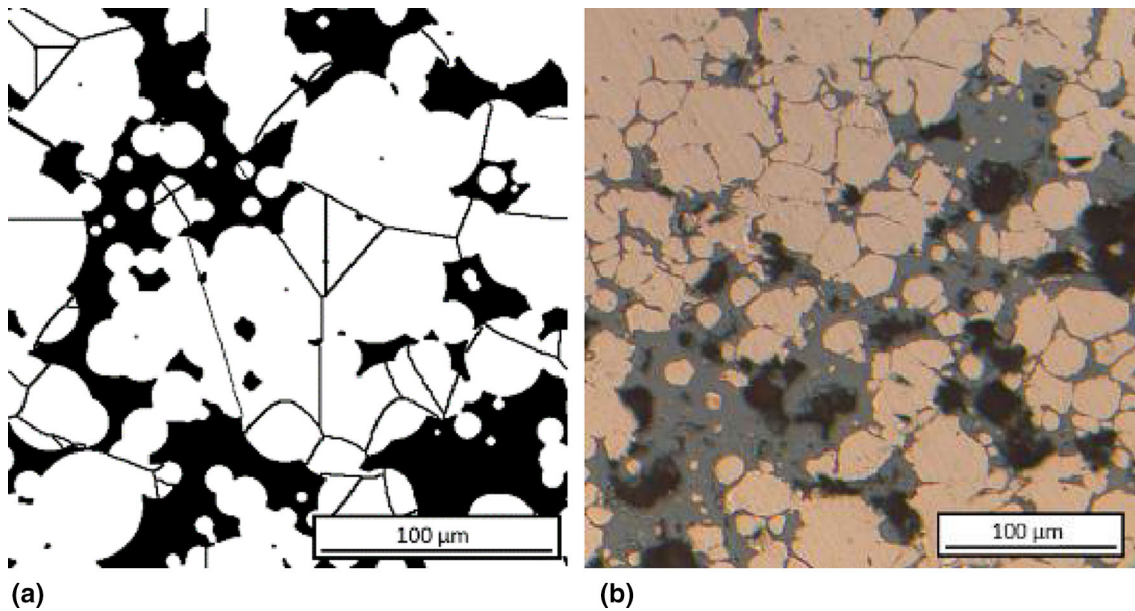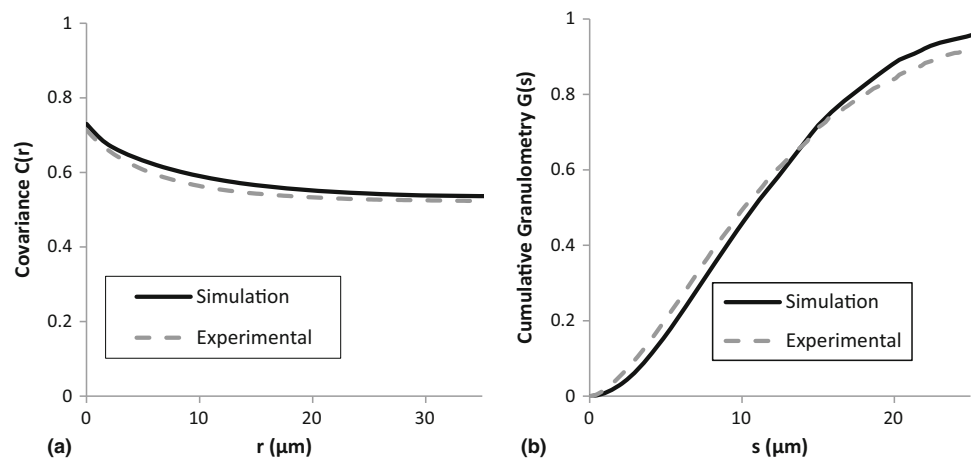
Fig. 12 Simulated (a) and experimental (b) images of a microstructure made of PEEK + non-oxidized copper

Fig. 13 Mean covariance and granulometry of experimental and simulated microstructures

optimized shape of the coating for this method is that of a cloverleaf. It is optimal because it concentrates current lines in the middle of the samples, thus forcing the current to follow a constant length path.

The Van der Pauw method requires a four-probe chamber connected to a source of current and an ohmmeter. Each probe was positioned on sample edges, as shown in Fig. 14. The current was applied between two probes, whereas the last two measured the resistance of the sample, after current stabilization. The four measurements, two for each direction, give two mean resistances, one for each direction. The conductivity σ could be computed by solving the Van der Pauw equation using the two mean resistances R_{13} and R_{24}:
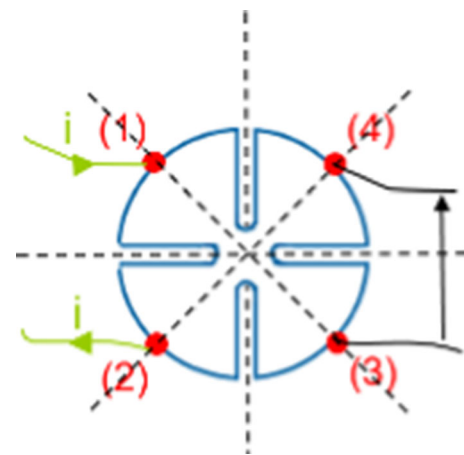
$$\sigma = \frac{2\ln 2}{\pi e(R_{13} + R_{24})} f$$

Fig. 14 Resistance measurement method using a cloverleaf sample

With e the thickness of each coating and f a shape factor, computed from:

$$\cosh\left\{\frac{\frac{R_{13}}{R_{24}} - 1}{\frac{R_{13}}{R_{24}} + 1}\frac{\ln 2}{f}\right\} = \frac{1}{2}e^{\frac{\ln 2}{f}}$$

If R_{13} equals R_{24}, the electrical resistivity of the coating is isotropic and f is 1.

The mean thickness e of the coatings was carefully measured by optical microscopy on 5 cross sections. Bulk copper exhibited an electric conductivity of 5.9×10^7 S m^{-1}, whereas PEEK reached 10^{-12} S m^{-1}.

The electrical conductivity of each sample was measured using the previously described Van der Pauw method in the current range of 1 mA, 10 mA, 100 mA, 500 mA and 1 A. Coatings were sprayed through a mask to obtain a cloverleaf shape with a diameter of 20 mm, as shown in Fig. 14. The conductivity as measured for each sample is displayed in Fig. 15 on a logarithmic scale. Several observations can be made from these measurements. First, the coating conductivity containing spherical non-oxidized copper greatly exceeds that of the coatings with irregular copper. Second, the current intensity seems to have a low influence on the global conductivity of the coatings, which mostly increases at 1 A. Coatings with irregular copper particles tend to burn at 1 A, as evidenced by dark marks in the current path, as shown in Fig. 16. Consequently, they are not suitable for current intensities higher than 0.5 A.

The results showed that the thinner was the coating, the higher was the conductivity, whatever its content and morphology. The highest conductivities for the coatings with non-oxidized spherical copper and irregular copper reach, respectively, 2×10^5 S m^{-1} and 2×10^3 S m^{-1}. These values have to be compared to the 5.9×10^7 S m^{-1} of the bulk copper.

To assess the influence of the cold spray process on the conductivity of pure copper coatings, a spherical non-oxidized coppe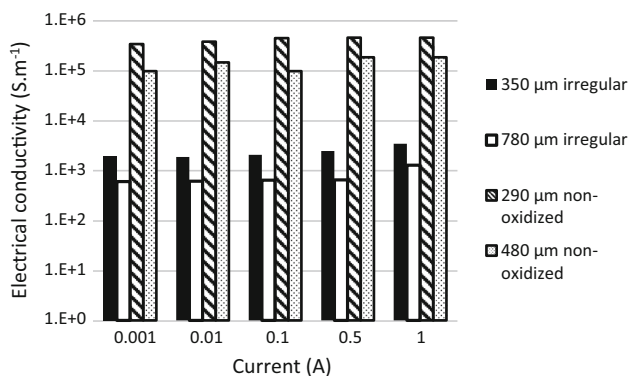r was sprayed directly onto PEEK substrates, as shown in Fig. 17. Conductivity measurements were applied to two samples using the Van der Pauw method. However, due to their high conductivity, the exact value was highly dependent on the coating thickness, which could greatly depend on the measuring method and on the considered part of the coating; i.e., the dense part only or the whole coating, as shown in Fig. 17. For these two coatings, two thickness measurement methods were considered: cross section observation or profilometry, as shown in Fig. 18. When considering the mean value of the thickness of the dense part of these coatings, the conductivity reached 7×10^7 S m^{-1}, a value higher than the copper bulk conductivity, which is impossible. On these two copper coatings, the conductivity also decreases when the thickness increases, but far less than for heterogeneous coatings, respectively, as shown in Figs. 15 and 18.

Discussion

The heterogeneous coatings hardly reached 10^5 S m^{-1}, which is two decades lower than the electric conductivity of bulk copper. Moreover, it was achieved using a mix of 80 vol.% of spherical non-oxidized copper particles with 20 vol.% of PEEK. Microstructural observations and materials properties suggest that the low effective conductivity is a consequence of the morphology of the microstructures.

Due to its ductility, PEEK is highly deformed upon impacts of hard copper particles at the processing temperature. Eventually, the former will partially cover the copper particles, limiting contacts between particles. Since PEEK is a dielectric material, it has a strong lowering effect on the conductivity of the whole coating as it prevents the current to flow between particles. A small volume
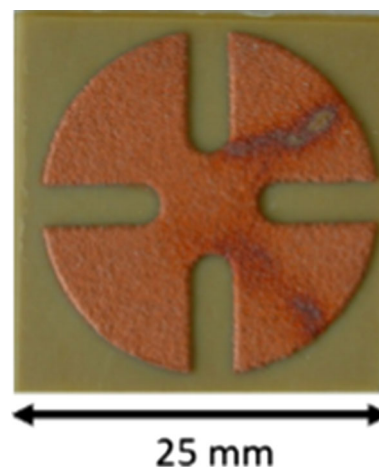

Fig. 15 Electric conductivity of the coatings under various current intensities

Fig. 16 Optical top view of an irregular copper–PEEK coated PEEK cloverleaf sample after resistance measurement under 1A

Fig. 17 Optical microscope image of a cross section of cold-sprayed copper coating onto PEEK
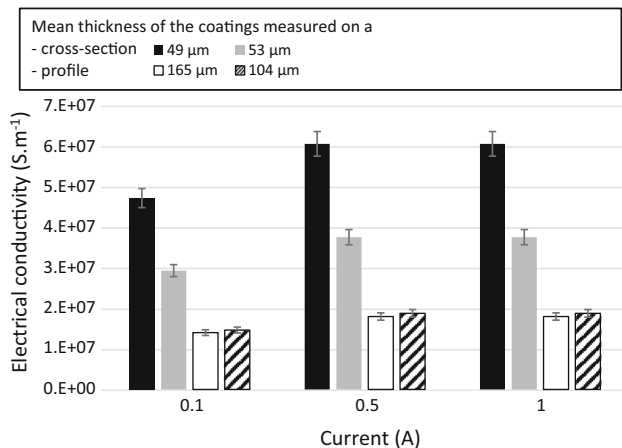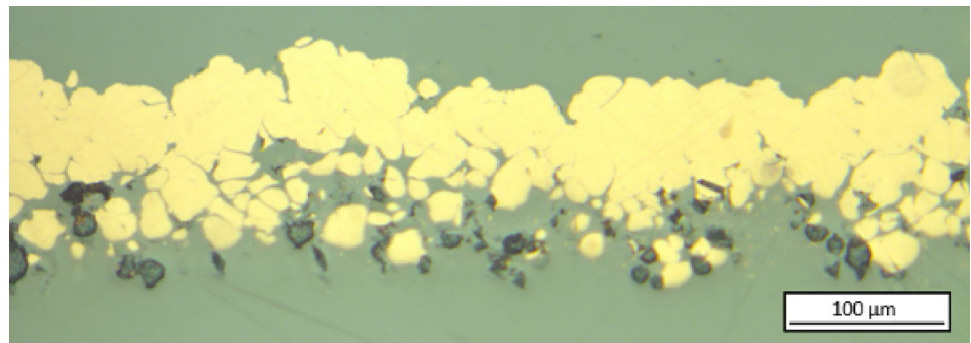

Fig. 18 Influence of copper coating thickness on conductivity

of PEEK in the powder feedstock has accordingly a severe impact on the conductivity of the whole coating. The PEEK greatly enhances the coating buildup on the CFRP substrate, but its volume in the feedstock and the shape of the particles should be monitored and controlled to prevent the previous effects.

Moreover, the analysis of the microstructures reveals that the latter contain in fact about 70 vol.% of copper, so that a volume of around 10% of copper has been lost during spraying. It is also worth noting that the highest conductivity is reached using powders with low surface oxidation. This observation suggests better contacts between particles, as well as inter-particles bonding with high copper content. We discuss these points in more details hereafter.

The cold spray parameters have been optimized to achieve a high deposition efficiency. The highest coating surface mass (considered to be proportional to the deposition efficiency) was obtained at 1.5 MPa and 400°C, this value being supposedly a good temperature/pressure compromise for building up the heterogeneous coating. Electrical properties, however, are induced by the copper phase, which suggest that a balance between copper content and coating buildup must be found.

The standard copper spraying parameters is, in fact, assumed to be 2.0 MPa and 400°C. Indeed, when spraying

heterogeneous coatings with the optimized parameters (1.5 MPa and 400°C), it was assumed that many particles rebounded due to their velocity being far from the critical velocity of copper. However, at higher temperature and pressure (1.5 MPa and 500°C), the surface mass felt of 43% at which point it is difficult to form continuous coatings (low buildup). Even if the coatings would contain more copper due to the higher velocity of the particles, they might present surface heterogeneity, which is unacceptable for electric application. The parameters were actually optimized to achieve the best acceptable copper content, better control of the coating buildup, so as to reduce thickness without leaving any uncoated zone.

To promote the anchoring of the copper particles without modifying spraying parameters, one may rely on the use of irregular shaped particles. Unfortunately, a whole range of coatings using the optimized parameters could not be achieved due to the technical limitations of the spraying facilities. A lower-pressure device able to quickly reach and spray steadily at 1.5 MPa and 500°C should be considered. We did not investigate coating microstructures obtained with these process parameters, but they may provide higher content of copper or better contacts. The coatings obtained and analyzed with irregular copper particles showed a high content of copper, less PEEK interstices, more plastic deformation and apparently more contacts than with oxidized particles, but a low conductivity. Actually, the achievement of irregular powders did correspond to some oxidation. These powders exhibited an oxide content of 2000 ppm. Even with a higher deformation, this limited chemical bonding between particles, which lowered the electrical conductivity. These particles could be deoxidized as presented by Malachowska et al. (Ref 10) to promote copper content, plastic deformation and bonding as observed in the case of spherical non-oxidized particles.

A morphological investigation confirmed these assumptions. Oxidized particles may be observed in the aggregates even after plastic deformation. This is not so for non-oxidized particles, none of which could be identified since most of their borders no longer exist after bonding
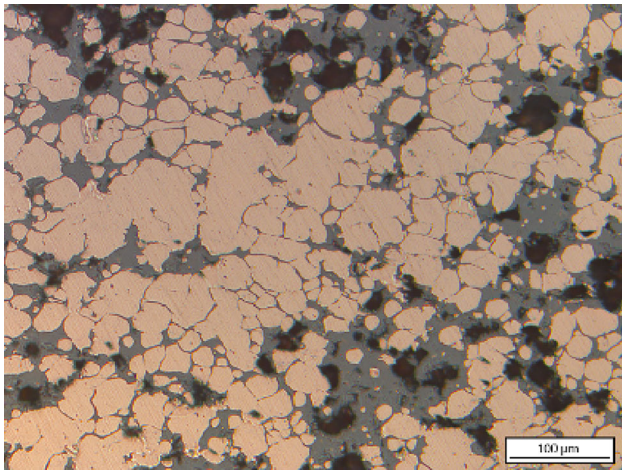
Fig. 19 Optical image (cross section) of a heterogeneous coating made of non-oxidized copper particles

(see Fig. 19). Quantitatively, the characteristics extracted from the images did not highlight real differences between coatings, see Table 4. This is due to the images resolution. The images wide scale is useful for calibrating the morphological model since it involves a large number of particles and however does not allow one to detect or segment particle interstices, especially thin ones. Despite optimization to work on microstructures with thin interstices (irregular and non-oxidized powders), poor electrical conductivity was obtained in comparison with microstructures containing oxidized particles. Larger images or a different cross section preparation, e.g., the use chemical etching, may help to highlight interstices.

An investigation of the microstructure in three dimensions could be helpful to study the material's macroscopic conductivity but requires careful selection of the x-ray microtomography device and parameters calibration. Two tests were performed on two installations, one leading to an image without contrast, because copper absorbs most of the energy, the other that renders PEEK burn due to high energy. Finally, these brittle coatings had to be debonded from the substrate and prepared carefully to achieve practicable samples. Morphological modeling of the microstructure in 3D is an alternative choice which allowed to reproduce coating microstructures at low cost. The numerical implementation of the model required significant development in order to produce large microstructures. The resulting model mimic coatings made of spherical oxidized particles with rather low deformation. The spheres generation was not fully adapted to simulate aggregates, as observed in the case of non-oxidized particles (Fig. 12). However, the use of spheres is sufficient to recover the covariance and granulometry of the material (Fig. 13). The method nevertheless highlights that these two criteria do not give a complete description of the experimental images. In particular, a detailed description of the interstice's shape and distribution is missing. A more complete modeling and simulation of coatings microstructure is presented in (Ref 27).

It would useful to investigate the effect of size and shape of particles on the coating effective electric conductivity. Simulated microstructures were optimized to visually and morphologically fit experimental ones. "Fast Fourier Transform" (FFT) full-field numerical procedures may be applied on simulated microstructures to determine numerically the effective electric conductivity of the simulated volumes. These results may be compared to experimental measurements to validate the method. A surface analysis of cross sections of the samples provided by an atomic-force microscope could be used to provide conductivity maps of the microstructures (Ref 28) and compared with FFT maps.

Conclusion

It has been shown in this work that cold spray is a suitable process to add electrically conductive metallic layers onto CFRP. The present approach relies on composite coatings of a metallic network of hard particles embedded in a soft matrix of polymer. The latter grows from CFRP, i.e., another soft matrix plus brittle carbon fibers. This led to highly heterogeneous, i.e., composite, microstructures, which could be improved by carefully selecting the copper powders on properties like shape, size and oxidation. The absence of oxide on the surface on the particles was highlighted as a key parameter to obtain a good conductivity as it enhanced the ability of the copper powder to deform and allowed particles to bond together. As a consequence, the coating is electrically conducting.

Using optimized cold spray parameters, a metal–polymer coating with a conductivity reaching 2×10^5 S m^{-1}, i.e., two decades below that of bulk copper, could be achieved, despite the presence of 30 vol.% of highly-insulating PEEK. Further work may focus on conductivity improvement through microstructure optimization, powder selection and cold spray parameters. In addition, thinner coatings may be targeted. These results are a useful step for producing coatings that may withstand a lightning strike with limited damages.

References

1. A. Sturgeon, B. Dunn, S. Celotto, and W. O'Neill, Cold Sprayed Coatings for Polymer Composite Substrate, *ESA SP*, 2006, **616**, p 1-5

2. X.L. Zhou, A.F. Chen, J.C. Liu, X.K. Wu, and J.S. Zhang, Preparation of Metallic Coatings on Polymer Matrix Composites by Cold Spray, *Surf. Coat. Technol.*, 2011, **206**(1), p 132-136

3. J. Affi, H. Okazaki, M. Yamada, and M. Fukumoto, Fabrication of Aluminum Coating onto CFRP Substrate by Cold Spray, *Mater. Trans.*, 2011, **9**(52), p 1759-1763

4. F.C. Campbell, *Structural composite materials*, Cleveland, ASM international, 2010

5. A. Ganesan, M. Yamada, and M. Fukumoto, Cold Spray Coating Deposition Mechanism on the Thermoplastic and Thermosetting Polymer Substrates, *J Therm Spray Technol*, 2013, **22**(8), p 1275-1282

6. R. Lupoi and W. O'Neill, Deposition of Metallic Coatings on Polymer Surfaces Using Cold Spray, *Surf. Coat. Technol.*, 2010, **205**(7), p 2167-2173

7. Giraud, D., F. Borit, V. Guipont, M. Jeandin, J. M. Malhaire, in Metallization of a polymer using cold spray: application to aluminum coating of polyamide 66. *Thermal Spray 2012: Proceedings of the International Thermal Spray Conference, Air, Land, Water, and the Human Body: Thermal Spray Science and Applications*, 21–24, 2012 (Houston, Texas, Springer 2013).

8. H. Che, X. Chu, P. Vo, and S. Yue, Metallization of Various Polymers by Cold Spray, *J. Therm. Spray Technol.*, 2018, **27**(1–2), p 169-178

9. C. Chen, X. Xie, Y. Xie, X. Yan, C. Huang, S. Deng, R. Zhongming, and H. Liao, Metallization of Polyether Ether Ketone (PEEK) by Copper Coating Via Cold Spray, *Surf. Coat. Technol.*, 2018, **342**, p 209-219

10. A. Małachowska, M. Winnicki, Ł. Konat, T. Piwowarczyk, L. Pawłowski, A. Ambroziak, and M. Stachowicz, Possibility of Spraying of copper Coatings on Polyamide 6 with Low Pressure Cold Spray Method, *Surf. Coat. Technol.*, 2017, **318**, p 82-89

11. A. Rezzoug, S. Abdi, A. Kaci, and M. Yandouzi, Thermal Spray Metallisation of Carbon Fibre Reinforced Polymer Composites: Effect of Top Surface Modification on Coating Adhesion and Mechanical Properties, *Surf. Coat. Technol.*, 2018, **333**, p 13-23

12. G. Archambault, B. Jodoin, S. Gaydos, and M. Yandouzi, Metallization of Carbon Fiber Reinforced Polymer Composite by Cold Spray and Lay-Up Molding Processes, *Surf. Coat. Technol.*, 2016, **300**, p 78-86

13. H. Che, P. Vo, and S. Yue, Metallization of Carbon Fibre Reinforced Polymers by Cold Spray, *Surf. Coat. Technol.*, 2017, **313**, p 236-247

14. H. Che, X. Chu, P. Vo, and S. Yue, Cold Spray of Mixed Metal Powders on Carbon Fibre Reinforced Polymers, *Surf. Coat. Technol.*, 2017, **329**, p 232-243

15. M. Jeandin, F. Borit, V. Guipont, L. Decker, D. Jeulin, M. Suzuki, and S. Sodeoka, Lattice Gas Modelling in Thermal Spraying, *Surf. Eng.*, 1999, **15**(3), p 191-194

16. O. Amsellem, K. Madi, F. Borit, D. Jeulin, V. Guipont, M. Jeandin, E. Boller, and F. Pauchet, Two-Dimensional (2D) and Three-Dimensional (3D) Analyses of Plasma-Sprayed Alumina Microstructures for Finite-Element Simulation of Young's Modulus, *J. Mater. Sci.*, 2008, **43**(12), p 4091-4098

17. S. Beauvais, V. Guipont, M. Jeandin, D. Jeulin, A. Robisson, and R. Saenger, Study of the Porosity in Plasma-Sprayed Alumina Through an Innovative Three-Dimensional Simulation of the Coating Buildup, *Metall. Mater. Trans. A*, 2008, **39**(11), p 2711-2724

18. K. Bobzin, N. Kopp, T. Warda, and M. Öte, Determination of the Effective Properties of Thermal Spray Coatings using 2d and 3d Models, *J. Therm. Spray Technol.*, 2012, **21**(6), p 1269-1277

19. Delloro, F., M. Faessel, H. Proudhon, D. Jeulin, M. Jeandin, E. Meillot, L. Blanchi, in A morphological approach to the modelling of the cold spray process. *Thermal Spray 2014: Proceedings of the International Thermal Spray Conference*, 2014 (Barcelona, Spain, DVS, 2014), pp. 221–226

20. Vitrex plc, VICTREX® PEEK 450G datasheet, http://www.victrex.com (2019)

21. M. Faessel., M. Bilodeau, Smil simple morphological image library, Séminaire Performance et Généricité, LRDE (2014)

22. L.J. Van der Pauw, A Method of Measuring Specific Resistivity and Hall Effect of Discs of Arbitrary Shape, *Philips Res. Rep.*, 1958, **13**, p 1-9

23. B. Figliuzzi, D. Jeulin, M. Faessel, F. Willot, M. Koishi, and N. Kowatari, Modelling the Microstructure and the Viscoelastic Behaviour Of Carbon Black Filled Rubber Materials from 3D Simulations, *Technische Mechanik*, 2016, **32**(1–2), p 22-46

24. J.B. Gasnier, F. Willot, H. Trumel, B. Figliuzzi, D. Jeulin, and M. Biessy, A Fourier-Based Numerical Homogenization Tool for an Explosive Material, *Matériaux & Techniques*, 2015, **103**(3), p 308

25. B. Figliuzzi, Eikonal-Based Models of Random Tessellations, *Image Anal. Stereol.*, 2019, **38**(1), p 15-23

26. E.P. Mamunya, V.V. Davidenko, and E.V. Lebedev, Percolation Conductivity of Polymer Composites Filled with Dispersed Conductive Filler, *Polym. Compos.*, 1995, **16**(4), p 319-324

27. V. Bortolussi, B. Figliuzzi, F. Willot, M. Faessel, and M. Jeandin, Morphological Modeling of Cold Spray Coatings, *Image Anal. Stereol.*, 2018, **37**(2), p 145-158

28. I. Balberg, D. Azulay, D. Toker, and O. Millo, Percolation and Tunneling in Composite Materials, *Int. J. Mod. Phys. B*, 2004, **18**(15), p 2091-2121